ACS APPLIED MATERIALS & INTERFACES

Research Article

Cite This: ACS Appl. Mater. Interfaces 2017, 9, 42717−42722

www.acsami.org

Zn/V_2O_5 Aqueous Hybrid-Ion Battery with High Voltage Platform and Long Cycle Life

Ping Hu,[†,∥] Mengyu Yan,[†,‡,∥] Ting Zhu,[†] Xuanpeng Wang,[†] Xiujuan Wei,[†] Jiantao Li,[†] Liang Zhou,[*,†] Zhaohuai Li,[†] Lineng Chen,[†] and Liqiang Mai[*,†,§]

[†]State Key Laboratory of Advanced Technology for Materials Synthesis and Processing, Wuhan University of Technology, Wuhan 430070, China

[‡]Materials Science and Engineering Department, University of Washington, Seattle 98195-2120, United States

[§]Department of Chemistry, University of California, Berkeley, California 94720, United States

Supporting Information

ABSTRACT: Aqueous zinc-ion batteries attract increasing attention due to their low cost, high safety, and potential application in stationary energy storage. However, the simultaneous realization of high cycling stability and high energy density remains a major challenge. To tackle the above-mentioned challenge, we develop a novel Zn/V_2O_5 rechargeable aqueous hybrid-ion battery system by using porous V_2O_5 as the cathode and metallic zinc as the anode. The V_2O_5 cathode delivers a high discharge capacity of 238 mAh g^{-1} at 50 mA g^{-1}. 80% of the initial discharge capacity can be retained after 2000 cycles at a high current density of 2000 mA g^{-1}. Meanwhile, the application of a "water-in-salt" electrolyte results in the increase of discharge platform from 0.6 to 1.0 V. This work provides an effective strategy to simultaneously enhance the energy density and cycling stability of aqueous zinc ion-based batteries.

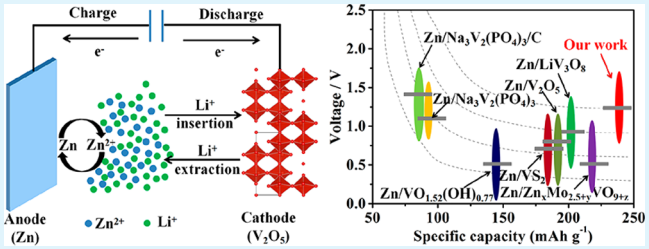

KEYWORDS: *vanadium pentoxide, aqueous hybrid-ion battery, high voltage platform, high energy density, "water-in-salt" electrolyte*

INTRODUCTION

Aqueous zinc-ion batteries (ZIBs) have attracted significant scientific and technical interests due to their high safety, colossal ionic conductivity, and high rate performance.[1−10] A series of ZIB cathode materials, including manganese-based materials,[2,6−8] Prussian blue,[9,11−13] and vanadium-based materials,[14,15] have been developed. Among these cathode materials, MnO_2 was reported first. However, the MnO_2 cathode suffers from significant capacity fading in aqueous electrolyte. The low capacity and poor cycle life limit its practical application. Recently, a series of new Mn-based nanomaterials have been reported to improve the energy density and cycling performance of ZIBs. Kang's group assembled a battery with an α-MnO_2 cathode and $ZnSO_4/Zn(NO_3)_2$ aqueous electrolyte, and the α-MnO_2 can deliver a high discharge capacity of 210 mAh g^{-1}.[3] Liu et al. adopted a $MnSO_4$ electrolyte additive in aqueous Zn/MnO_2 battery to suppress the dissolution of Mn^{2+} and achieved significantly improved energy density and cycling stability.[7] For Prussian blue, the limited capacity (∼50 mAh g^{-1}) and O_2 evolution at a high operating voltage hinder its practical applications.

Vanadium-based materials are very attractive for aqueous ZIBs due to the advantages of abundant resources, low cost, and good safety.[14−25] He et al. reported a VS_2 cathode material for ZIBs. The VS_2 cathode exhibited a high specific discharge capacity of 190.3 mAh g^{-1} and long-term cyclic stability.[14] Nazar's group reported a vanadium oxide bronze pillared by Zn^{2+} and crystalline water ($Zn_{0.25}V_2O_5{\cdot}nH_2O$), which demonstrated a capacity retention of more than 80% after 1000 cycles.[15] However, the voltage platform of the vanadium-based cathodes (VS_2, $Zn_{0.25}V_2O_5{\cdot}nH_2O$, LiV_3O_8...) for ZIBs is not high enough, resulting in less competitive advantages in energy density.

Recently, it has been demonstrated that "water-in-salt" electrolyte is able to retard the hydrogen and oxygen evolution at a high electrochemical window in aqueous electrolyte (∼3.0 V).[26−31] Xu et al. first constructed a full aqueous Li-ion battery with $LiMn_2O_4$ cathode, Mo_6S_8 anode, and 21 m lithium bis(trifluoromethane sulfonyl)imide (LiTFSI) as the electrolyte; such an aqueous battery demonstrated an open-circuit voltage of 2.3 V.[26] Since then, a series of "water-in-salt" electrolytes have been reported for aqueous ion batteries, enabling relatively high voltage and energy density.[27−31] Chen et al. assembled a $Zn/LiMn_{0.8}Fe_{0.2}PO_4$ aqueous hybrid-ion battery based on a "water-in-salt" electrolyte, which obtained a high energy density of 183 Wh kg^{-1} and a high operating voltage exceeding 1.8 V.[32] Given that the use of "water-in-salt" electrolyte can enhance the energy density of aqueous metal ion

Received: August 30, 2017
Accepted: November 20, 2017
Published: November 20, 2017

DOI: 10.1021/acsami.7b13110
ACS Appl. Mater. Interfaces 2017, 9, 42717−42722

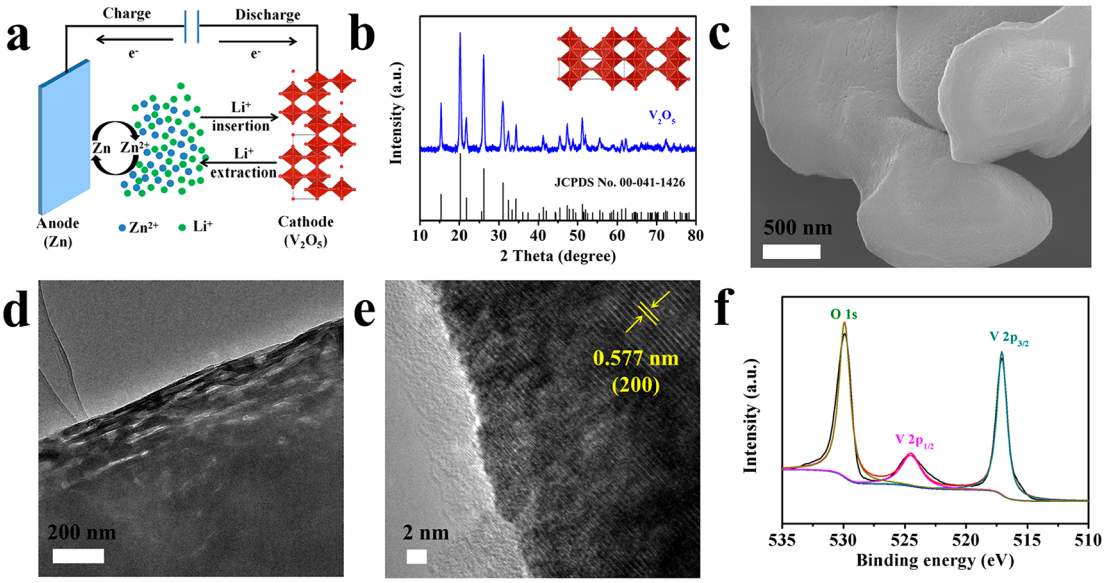

Figure 1. (a) Schematic illustration of a Zn/V_2O_5 aqueous hybrid-ion battery, (b) X-ray diffraction pattern, (c) FESEM image, (d) TEM image, (e) HRTEM image, and (f) high-resolution XPS spectrum of porous V_2O_5.

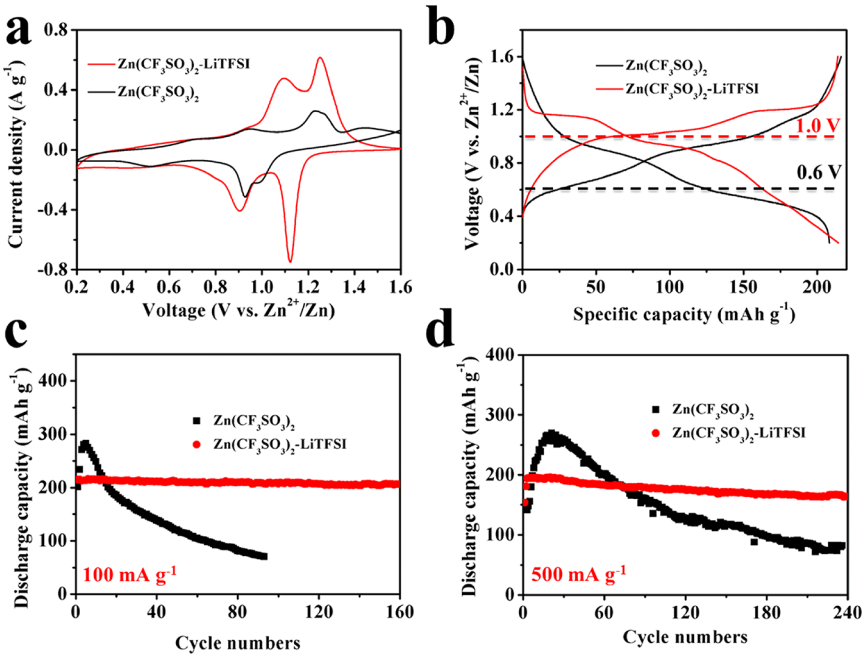

Figure 2. Electrochemical performances of the porous V_2O_5 in $Zn(CF_3SO_3)_2$−LiTFSI "water-in-salt" electrolyte and $Zn(CF_3SO_3)_2$ electrolyte. (a) CV curves of Zn/V_2O_5 batteries at 0.1 mV s^{-1}. (b) The 15th cycle charge/discharge curves of Zn/V_2O_5 batteries at 100 mA g^{-1}. Cycling stability of the V_2O_5 at 100 (c) and 500 (d) mA g^{-1}.

batteries, the extension of "water-in-salt" electrolyte in aqueous Zn/vanadium-based material batteries may give rise to a higher energy density as well.

Herein, we designed a novel Zn/V_2O_5 aqueous hybrid-ion battery (Figure 1a) with "water-in-salt" electrolyte (21 m LiTFSI and 1 m $Zn(CF_3SO_3)_2$). The employment of this strategy can lead to great improvements in both voltage platform and cycling stability. The porous V_2O_5 cathode exhibits a high discharge capacity (238 mAh g^{-1} at 50 mA g^{-1}), superior rate capability (156 mAh g^{-1} at 1000 mA g^{-1}), and long-term cyclability (80% capacity retention after 2000 cycles at 2000 mA g^{-1}) based on the "water-in-salt" electrolyte. Our study highlights that the employment of "water-in-salt" electrolyte is an effective way to boost the energy density and cyclability of aqueous zinc ion-based batteries.

RESULTS AND DISCUSSION

The porous V_2O_5 microplates are synthesized via a simple organics-assisted strategy. The X-ray diffraction (XRD) pattern of the porous V_2O_5 prepared at 350 °C clearly displays a high degree of crystallization. All the diffraction peaks of the prepared sample can be assigned to orthorhombic V_2O_5 (JCPDS 41-1426) (Figure 1b).[16] Field-emission scanning electron microscopic (FESEM) images show that the V_2O_5 exhibits a quasi-hexagonal microplate morphology with plenty of mesopores (Figures 1c and S1a−d). The highly porous

DOI: 10.1021/acsami.7b13110
ACS Appl. Mater. Interfaces 2017, 9, 42717−42722

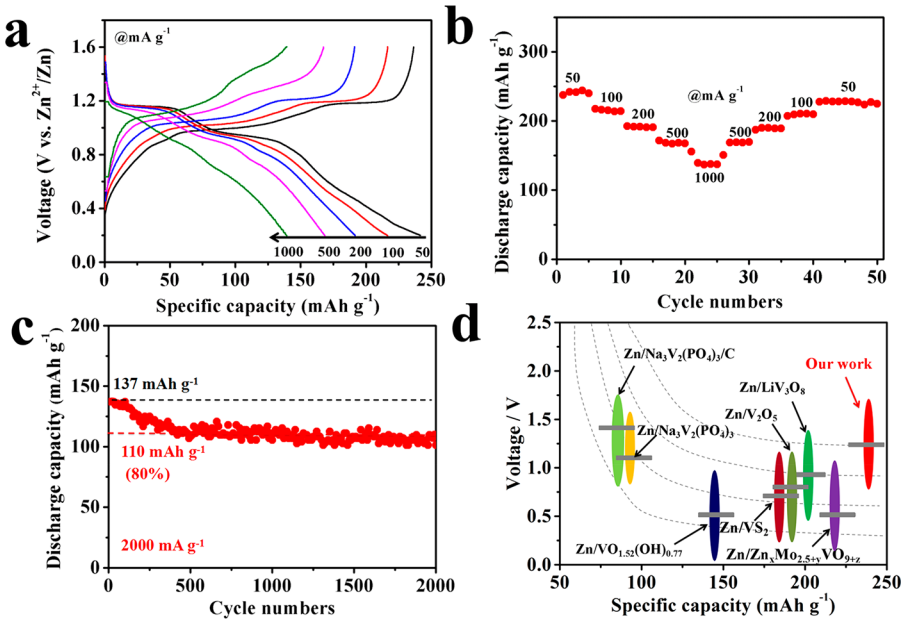

Figure 3. Electrochemical performance of the porous V_2O_5 in $Zn(CF_3SO_3)_2$−LiTFSI "water-in-salt" electrolyte. (a,b) Charge/discharge curves and rate performance of the V_2O_5 at various current densities ranging from 50 to 1000 mA g^{-1}, respectively. (c) Long-term cycling stability of the V_2O_5 at 2000 mA g^{-1}. (d) Comparison of porous V_2O_5 with recently reported vanadium-based cathode for zinc-ion batteries in terms of specific capacity and voltage platform.

feature of V_2O_5 can be further confirmed by transmission electron microscopy (TEM) as shown in Figure 1d. The lattice spacing of 0.577 nm matches well with the interplanar distance of the (200) plane (Figure 1e). To investigate the valence states of V and O in the V_2O_5, the X-ray photoelectron (XPS) spectrum of the V_2O_5 is shown in Figure 1f. For the V 2p spectrum, the binding energies for V $2p_{1/2}$ and V $2p_{3/2}$ are located at 524.7 and 517.0 eV, respectively, matching well with those of V_2O_5.[33,34] For the O 1s spectrum, the binding energy is 530.0 eV, in good agreement with that of V_2O_5.[34] The porous V_2O_5 exhibits a high specific surface area of 14.7 m^2 g^{-1}, which is measured by nitrogen sorption (Figure S2).

The cyclic voltammogram (CV) curves collected in different electrolytes at 0.1 mV s^{-1} are shown in Figure 2a and Figure S3. In $Zn(CF_3SO_3)_2$ (Figure 2a), three reduction peaks (0.52, 0.93, and 0.98 V) and four oxidation peaks (0.71, 0.95, 1.22, and 1.43 V) can be observed in the second CV curve, which are caused by the zinc ion intercalation/deintercalation during the discharge/change processes. In LiTFSI (Figure S3), three pairs of cathodic/anodic peaks can be observed at 0.56/0.90 V, 0.95/1.08 V, and 1.17/1.22 V, which are associated with Li^+ insertion/extraction in the V_2O_5. In $Zn(CF_3SO_3)_2$−LiTFSI, two pairs of redox peaks appear at 0.90/1.08 V and 1.12/1.25 V, which is similar to the result obtained in LiTFSI to some extent. This suggests that the lithium ions may actually be involved in the electrochemical processes of Zn/V_2O_5 batteries with hybrid $Zn(CF_3SO_3)_2$−LiTFSI electrolyte.

When 1 m $Zn(CF_3SO_3)_2$ is used as the electrolyte, the Zn/V_2O_5 battery shows unstable charge/discharge plateaus and cycling performance (Figure S4a). In sharp contrast, quite stable working plateaus and cyclability can be achieved when $Zn(CF_3SO_3)_2$−LiTFSI "water-in-salt" electrolyte is used (Figure S4b). The Zn/V_2O_5 battery with $Zn(CF_3SO_3)_2$−LiTFSI electrolyte shows two pairs of charge (1.06 and 1.23 V) and discharge (0.90 and 1.10 V) plateaus, which are much higher than those with $Zn(CF_3SO_3)_2$ electrolyte (Figure 2b). In addition, the overpotential of the Zn/V_2O_5 battery with $Zn(CF_3SO_3)_2$−LiTFSI is lower than that with $Zn(CF_3SO_3)_2$. This is because the Li^+ intercalation/deintercalation in $Zn(CF_3SO_3)_2$−LiTFSI is more feasible than the Zn^{2+} insertion/extraction in $Zn(CF_3SO_3)_2$. The working voltage is also increased when a low-concentration LiTFSI electrolyte (1 m) was used. However, it is not stable during the charge/discharge processes and the capacity fades quickly (Figure S5).

The porous V_2O_5 delivers an initial discharge capacity of 215 mAh g^{-1} at 100 mA g^{-1} in $Zn(CF_3SO_3)_2$−LiTFSI with a high Coulombic efficiency (CE) of 97% (Figure S6), indicating a highly reversible ion insertion/extraction process (Figure 2c). After 160 cycles, 95% (204 mAh g^{-1}) of the highest capacity can be maintained, demonstrating the excellent cycling stability. In 1 m $Zn(CF_3SO_3)_2$, the V_2O_5 delivers an initial discharge capacity of 201 mAh g^{-1}. The capacity increases to 292 mAh g^{-1} at the first fifth, after which the capacity decreases continuously to 73 mAh g^{-1} after 90 cycles. When cycled in 21 m LITFSI, the V_2O_5 exhibits an initial discharge capacity of 178 mAh g^{-1} (Figure S7). However, the capacity fades quickly with cycling, and only 58% of the initial capacity is retained after 50 cycles. A possible reason for the poor cyclability of V_2O_5 in 21 m LiTFSI is the lack of Zn ions, making the electrodeposition of Zn on anode during the charge process difficult. The cycling performance of the battery in $Zn(CF_3SO_3)_2$−LiTFSI electrolyte with both lithium and zinc ions outperforms that in either $Zn(CF_3SO_3)_2$ or LiTFSI electrolyte, implying a synergistic effect may exist in the Zn/V_2O_5 battery with $Zn(CF_3SO_3)_2$−LiTFSI.

At a high current density of 500 mA g^{-1}, 85% of the initial discharge capacity of the V_2O_5 in $Zn(CF_3SO_3)_2$−LiTFSI can be retained after 240 cycles (Figure 2d), while for V_2O_5 in $Zn(CF_3SO_3)_2$, only 58% of the initial capacity was retained. The CE also differs significantly. With $Zn(CF_3SO_3)_2$−LiTFSI electrolyte, the CE stabilizes in the range of 99−101%, and with

DOI: 10.1021/acsami.7b13110
ACS Appl. Mater. Interfaces 2017, 9, 42717−42722

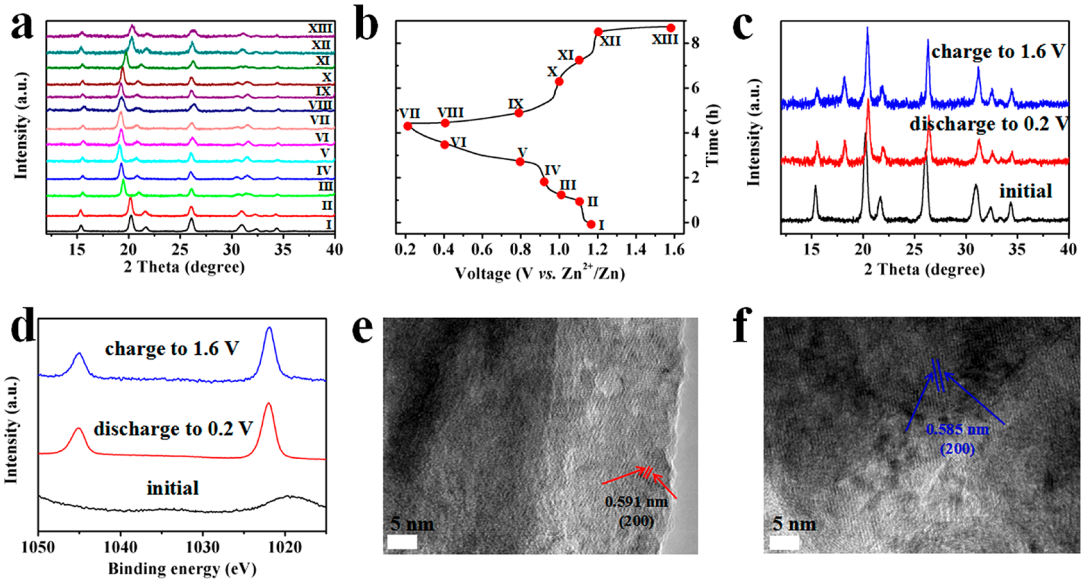

Figure 4. (a,b) XRD patterns of the V_2O_5 cathode in a Zn/V_2O_5 battery with $Zn(CF_3SO_3)_2$–LiTFSI collected at various states at 100 mA g^{-1}. (c) *Ex-situ* XRD patterns collected at different electrochemical states in $Zn(CF_3SO_3)_2$ electrolyte (black: initial state, red: discharged to 0.2 V; blue: charged to 1.6 V) at 100 mA g^{-1}. (d) *Ex-situ* XPS collected at different electrochemical states in $Zn(CF_3SO_3)_2$–LiTFSI electrolyte at 100 mA g^{-1}. (e,f) *Ex-situ* TEM images at discharged (e) and charged (f) states in $Zn(CF_3SO_3)_2$–LiTFSI electrolyte at 100 mA g^{-1}.

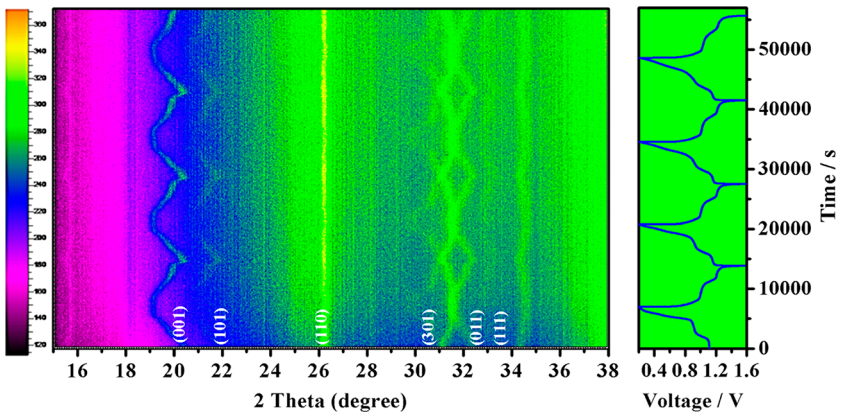

Figure 5. *In-situ* XRD patterns collected during galvanostatic charge/discharge: image plot of the diffraction patterns of the V_2O_5 in $Zn(CF_3SO_3)_2$–LiTFSI at 15–38° during the charge/discharge cycles at 100 mA g^{-1}.

$Zn(CF_3SO_3)_2$, the CE fluctuates between 97% and 115% (Figure S6).

The porous V_2O_5 in $Zn(CF_3SO_3)_2$–LiTFSI (Figure 3a, b) also exhibits better rate capability than that in $Zn(CF_3SO_3)_2$ (Figure S8). In $Zn(CF_3SO_3)_2$–LiTFSI, the porous V_2O_5 delivers high capacities of 242, 217, 192, 171, and 156 mAh g^{-1} at 50, 100, 200, 500, and 1000 mA g^{-1}, respectively (Figure 3b). When the current density returns to 50 mA g^{-1}, about 88% of the initial discharge capacity can be regained. After 50 cycles, a discharge capacity of 213.4 mAh g^{-1} can be retained, which is much higher than the capacity of V_2O_5 in $Zn(CF_3SO_3)_2$ (79 mAh g^{-1}, Figure S8). Electrochemical impedance spectroscopy (EIS) characterization was also carried out. The formation of thicker and more protective solid electrolyte interphase (SEI) layer in LiTFSI–$Zn(CF_3SO_3)_2$ leads to lower electrical conductivity and ion diffusion than that in $Zn(CF_3SO_3)_2$ (Figure S9).[27]

The excellent cycling stability at high rate is the most appealing property of the Zn/V_2O_5 aqueous hybrid-ion battery. At a high current density of 2000 mA g^{-1}, 80% of the initial capacity can be retained after 2000 cycles (Figure 3c). From the above results, it is safe to conclude that the employment of $Zn(CF_3SO_3)_2$–LiTFSI "water-in-salt" electrolyte greatly improves the cycling stability and energy density of the Zn/V_2O_5 batteries. To the best of our knowledge, the Zn/V_2O_5 shows one of the most promising electrochemical performances in terms of combined high rate capability and long-term cycling stability. Most importantly, when compared to the recently reported vanadium-based ZIB cathode materials, the porous V_2O_5 manifests one of the highest capacities with moderately high voltage platforms (Figure 3d),[5,14,20−24] demonstrating the great potential for energy storage applications.

To monitor the structural change of porous V_2O_5 in different electrolytes during the charge/discharge processes, *ex-situ* XRD experiments were carried out. The V_2O_5 in $Zn(CF_3SO_3)_2$–LiTFSI behaves quite differently from that in $Zn(CF_3SO_3)_2$. In hybrid $Zn(CF_3SO_3)_2$–LiTFSI electrolyte, the (001) diffraction peak, which is originally located at 20.2°, shifts toward lower angles at the initial discharge process and then shifts back to its original position in the subsequent charge process, indicating

DOI: 10.1021/acsami.7b13110
ACS Appl. Mater. Interfaces 2017, 9, 42717−42722

the highly reversible expansion/extraction of the corresponding lattice distance (Figure 4a, 4b).[35−37] In $Zn(CF_3SO_3)_2$, the (001) diffraction located at ∼20.2° and (110) diffraction located at ∼26.2° shift toward higher angles during the discharge process (Figure 4c). Both peaks shift toward lower angles slightly during the subsequent charge process; however, neither of them can recover to their initial positions. In addition, a new peak appears at 18.2° during the initial discharge, and it does not disappear upon charge. The *ex-situ* XRD results demonstrate that the V_2O_5 in $Zn(CF_3SO_3)_2$ suffers from serious irreversible structural change during charge/discharge processes.

To investigate whether the Zn ions can insert into or extract from the V_2O_5 reversibly in $Zn(CF_3SO_3)_2$−LiTFSI, *ex-situ* XPS and TEM characterizations were carried out (Figure 4d−f). No signal of Zn can be detected in the XPS spectrum of V_2O_5 (Figure 4d). When discharged to 0.2 V, the Zn ions can be successfully intercalated into V_2O_5 as demonstrated by the obvious Zn 2p 3/2−1/2 spin−orbit doublet. However, not all the Zn ions can be deintercalated after recharging to 1.6 V. It is speculated that the trapped Zn ions may act as the interlayer pillars and stabilize the layered structure of V_2O_5 during the charge/discharge processes, which is similar to the effects of preintercalated metal ions (Li^+, Na^+, K^+, Zn^{2+}, ...) in V_2O_5.[15,38] The HRTEM images display a slight lattice spacing change of the (200) plane during the charge/discharge processes (Figure 4e, 4f). When discharged to 0.2 V, the (200) lattice spacing increases by 2.43% compared to that of the original state, confirming the intercalation reaction mechanism and agreeing well with the *ex-situ* XRD results.

To provide further insight into the structural change of the porous V_2O_5 in $Zn(CF_3SO_3)_2$−LiTFSI during charging and discharging, *in-situ* XRD was performed as well (Figure 5). The 2θ range is recorded from 15 to 38°, a range which can well reflect the structural changes of the V_2O_5. As observed in the *in-situ* XRD study, the (200) diffraction shifts leftwards and rightwards during discharge and charge, respectively. In addition, the (301) and (011) diffraction peaks merge into one peak during discharge, and the new peak splits into two peaks during charge. These changes are completely reversible during cycling, suggesting the highly reversible electrochemical reactions. Interestingly, the *in-situ* XRD results show great similarity to those of Li/V_2O_5 batteries in nonaqueous electrolyte ($LiPF_6$/EC/DEC = 1:1:1 vol/vol/vol),[39] implying the insertion and extraction of Li ions in V_2O_5 play a significant role in the Zn/V_2O_5 battery with $Zn(CF_3SO_3)_2$−LiTFSI electrolyte. Considering both the Zn ions and Li ions involved in the electrochemical processes of the Zn/V_2O_5 battery, we term it hybrid-ion batteries rather than ZIBs.

CONCLUSION

In conclusion, we develop a novel Zn/V_2O_5 rechargeable aqueous hybrid-ion battery. The application of $Zn(CF_3SO_3)_2$−LiTFSI "water-in-salt" electrolyte enables the Zn/V_2O_5 battery with high discharge platform and outstanding cycling performance. *In/ex-situ* characterizations demonstrate that both the Zn ions and Li ions are involved in the electrochemical processes. This work highlights that the hybrid "water-in-salt" electrolyte is a promising strategy to enhance the energy density and long-term cycling stability of zinc-ion-based aqueous batteries.

ASSOCIATED CONTENT

Supporting Information

The Supporting Information is available free of charge on the ACS Publications website at DOI: 10.1021/acsami.7b13110.

SEM images of V_2O_5; nitrogen sorption results of V_2O_5, CV curves of the V_2O_5 in LiTFSI and $Zn(CF_3SO_3)_2$−LiTFSI at the scan rate of 0.1 mV s^{-1}; charge/discharge curves at different cycles of Zn/V_2O_5 batteries with different electrolytes; Coulombic efficiency of the V_2O_5 cathode in $Zn(CF_3SO_3)_2$ and $Zn(CF_3SO_3)_2$−LiTFSI; cycling performance and Coulombic efficiency of the V_2O_5 cathode in 21 m LiTFSI; rate performance of V_2O_5 in $Zn(CF_3SO_3)_2$, AC impedance spectra of the V_2O_5 electrode in $Zn(CF_3SO_3)_2$ and $Zn(CF_3SO_3)_2$−LiTFSI (PDF)

AUTHOR INFORMATION

Corresponding Authors

*E-mail: liangzhou@whut.edu.cn.

*E-mail: mlq518@whut.edu.cn.

ORCID

Liang Zhou: 0000-0001-6756-3578

Liqiang Mai: 0000-0003-4259-7725

Author Contributions

[‖]P. Hu and M. Y. Yan contributed equally to this work. The manuscript was written through contributions of all authors. All authors have given approval to the final version of the manuscript.

Notes

The authors declare no competing financial interest.

ACKNOWLEDGMENTS

This work was supported by the National Key Research and Development Program of China (2016YFA0202603), the National Basic Research Program of China (2013CB934103), the Programme of Introducing Talents of Discipline to Universities (B17034), the National Natural Science Foundation of China (51521001, 21673171, 51502226), the National Natural Science Fund for Distinguished Young Scholars (51425204), the Fundamental Research Funds for the Central Universities (WUT: 2016III001, 2016III002), and State Key Laboratory of Advanced Technology for Materials Synthesis and Processing (WUT: 2017-KF-2). Prof. Liqiang Mai gratefully acknowledges financial support from China Scholarship Council (No. 201606955096). We thank Prof. Peidong Yang of University of California, Berkeley for strong support and stimulating discussions.

REFERENCES

(1) Yan, J.; Wang, J.; Liu, H.; Bakenov, Z.; Gosselink, D.; Chen, P. Rechargeable Hybrid Aqueous Batteries. *J. Power Sources* **2012**, *216*, 222−226.

(2) Zhu, X.; Wu, X.; Doan, T.; Tian, Y.; Zhao, H.; Chen, P. Binder-free Flexible $LiMn_2O_4$/carbon Nanotube Network as High Power Cathode for Rechargeable Hybrid Aqueous Battery. *J. Power Sources* **2016**, *326*, 498−504.

(3) Xu, C.; Li, B.; Du, H.; Kang, F. Energetic Zinc Ion Chemistry: the Rechargeable Zinc Ion Battery. *Angew. Chem., Int. Ed.* **2012**, *51*, 933−935.

(4) Zhang, L.; Chen, L.; Zhou, X.; Liu, Z. Towards High-voltage Aqueous Metal-ion Batteries Beyond 1.5 V: The Zinc/zinc Hexacyanoferrate System. *Adv. Energy Mater.* **2015**, *5*, 1400930.

(5) Alfaruqi, M.; Mathew, V.; Song, J.; Kim, S.; Islam, S.; Pham, D.; Jo, J.; Kim, S.; Baboo, J.; Xiu, Z.; Lee, K.; Sun, Y.; Kim, J. Electrochemical Zinc Intercalation in Lithium Vanadium Oxide: A High-capacity Zinc-ion Battery Cathode. *Chem. Mater.* **2017**, *29*, 1684−1694.

(6) Lee, J.; Ju, J.; Cho, W.; Cho, B.; Oh, S. Todorokite-type MnO_2 as A Zinc-ion Intercalating Material. *Electrochim. Acta* **2013**, *112*, 138−143.

(7) Pan, H.; Shao, Y.; Yan, P.; Cheng, Y.; Han, K.; Nie, Z.; Wang, C.; Yang, J.; Li, X.; Bhattacharya, P.; Muller, K.; Liu, J. Reversible Aqueous Zinc/manganese Oxide Energy Storage From Conversion Reactions. *Nat. Energy* **2016**, *1*, 16039.

(8) Lee, B.; Lee, H.; Kim, H.; Chung, K.; Cho, B.; Oh, S. Elucidating the Intercalation Mechanism of Zinc Ions into α-MnO_2 for Rechargeable Zinc Batteries. *Chem. Commun.* **2015**, *51*, 9265−9268.

(9) Liu, Z.; Pulletikurthi, G.; Endres, F. A Prussian Blue/zinc Secondary Battery with A Bio-ionic Liquid−water Mixture as Electrolyte. *ACS Appl. Mater. Interfaces* **2016**, *8*, 12158−12164.

(10) Kaveevivitchai, W.; Manthiram, A. High-capacity Zinc-ion Storage in An Open-Tunnel Oxide for Aqueous and Nonaqueous Zn-ion Batteries. *J. Mater. Chem. A* **2016**, *4*, 18737−18741.

(11) Alfaruqi, M.; Mathew, V.; Gim, J.; Kin, S.; Song, J.; Baboo, J.; Choi, S.; Kim, J. Electrochemically Induced Structural Transformation in A γ-MnO_2 Cathode of A High Capacity Zinc-ion Battery System. *Chem. Mater.* **2015**, *27*, 3609−3620.

(12) Zhang, L.; Chen, L.; Zhou, X.; Liu, Z. Morphology-dependent Electrochemical Performance of Zinc Hexacyanoferrate Cathode for Zinc-ion Battery. *Sci. Rep.* **2016**, *5*, 18263.

(13) Trócoli, R.; Mantia, F. An Aqueous Zinc-ion Battery Based on Copper Hexacyanoferrate. *ChemSusChem* **2015**, *8*, 481−485.

(14) He, P.; Yan, M.; Zhang, G.; Sun, R.; Chen, L.; An, Q.; Mai, L. Layered VS_2 Nanosheet-based Aqueous Zinc Ion Battery Cathode. *Adv. Energy Mater.* **2017**, *5*, 1601920.

(15) Kundu, D.; Adams, B.; Duffort, V.; Vajargah, S.; Nazar, L. A High-capacity and Long-life Aqueous Rechargeable Zinc Battery Using A Metal Oxide Intercalation Cathode. *Nat. Energy* **2016**, *1*, 16119.

(16) An, Q.; Zhang, P.; Wei, Q.; He, L.; Xiong, F.; Sheng, J.; Wang, Q.; Mai, L. Top-down Fabrication of Three-dimensional Porous V_2O_5 Hierarchical Microplates with Tunable Porosity for Improved Lithium Battery Performance. *J. Mater. Chem. A* **2014**, *2*, 3297−3302.

(17) Wang, X.; Niu, C.; Meng, J.; Hu, P.; Xu, X.; Wei, X.; Zhou, L.; Zhao, K.; Luo, W.; Yan, M.; Mai, L. Novel $K_3V_2(PO_4)_3$/C Bundled Nanowires as Superior Sodium-Ion Battery Electrode with Ultrahigh Cycling Stability. *Adv. Energy Mater.* **2015**, *5*, 1500716.

(18) Qiao, H.; Zhu, X.; Zheng, Z.; Liu, L.; Zhang, L. Synthesis of $V_3O_7{\cdot}H_2O$ Nanobelts as Cathode Materials for Lithium−ion Batteries. *Electrochem. Commun.* **2006**, *8*, 21−26.

(19) Li, G.; Yang, Z.; Jiang, Y.; Jin, C.; Huang, W.; Ding, X.; Huang, Y. Towards Polyvalent Ion Batteries: a Zinc-ion Battery Based on NASICON Structured $Na_3V_2(PO_4)_3$. *Nano Energy* **2016**, *25*, 211−217.

(20) Senguttuvan, P.; Han, S.; Kim, S.; Lipson, A.; Tepavcevic, S.; Fister, T.; Bloom, I.; Burrell, A.; Johnson, C. A High Power Rechargeable Nonaqueous Multivalent Zn/V_2O_5 Battery. *Adv. Energy Mater.* **2016**, *6*, 1600826.

(21) Kaveevivitchai, W.; Manthiram, A. High-capacity Zinc-ion Storage in An Open-Tunnel Oxide for Aqueous and Nonaqueous Zn-ion Batteries. *J. Mater. Chem. A* **2016**, *4*, 18737−18741.

(22) Jo, J.; Sun, Y.; Myung, S. Hollandite-type Al-doped $VO_{1.52}(OH)_{0.77}$ as A Zinc Ion Insertion Host Material. *J. Mater. Chem. A* **2017**, *5*, 8367−8375.

(23) Li, G.; Yang, Z.; Jiang, Y.; Zhang, W.; Huang, Y. Hybrid Aqueous Battery Based on $Na_3V_2(PO_4)_3$/C Cathode and Zinc Anode for Potential Large-scale Energy Storage. *J. Power Sources* **2016**, *308*, 52−57.

(24) Tang, H.; Xu, N.; Pei, C.; Xiong, F.; Tan, S.; Luo, W.; An, Q.; Mai, L. $H_2V_3O_8$ Nanowires as High Capacity Cathode Materials for Magnesium-based Battery. *ACS Appl. Mater. Interfaces* **2017**, *9*, 28667.

(25) Saravanakumar, B.; Kamatchi, K.; Purushothaman; Muralidharan, G. Interconnected V_2O_5 Nanoporous Network for High-performance Supercapacitors. *ACS Appl. Mater. Interfaces* **2012**, *4*, 4484−4490.

(26) Suo, L.; Borodin, O.; Gao, T.; Olguin, M.; Ho, J.; Fan, X.; Luo, C.; Wang, C.; Xu, K. "Water-in-salt" Electrolyte Enables High-voltage Aqueous Lithium-ion Chemistries. *Science* **2015**, *350*, 938−943.

(27) Suo, L.; Borodin, O.; Sun, W.; Fan, X.; Yang, C.; Wang, F.; Gao, T.; Ma, Z.; Schroeder, M.; Gresce, A.; Russell, S.; Armand, M.; Angell, A.; Xu, K.; Wang, C. Advanced High-voltage Aqueous Lithium-ion Battery Enabled by Water-in-Bisalt Electrolyte. *Angew. Chem., Int. Ed.* **2016**, *55*, 7136−7141.

(28) Gambou-Bosca, A.; Belanger, D. Electrochemical Characterization of MnO_2-based Composite in the Presence of Salt-in-water and Water-in-salt Electrolytes as Electrode for Electrochemical Capacitors. *J. Power Sources* **2016**, *326*, 595−603.

(29) Kühnel, R.; Reber, D.; Remhof, A.; Figi, R.; Bleiner, D.; Battaglia, C. "Water-in-salt" Electrolytes Enable the Use of Cost-effective Aluminum Current Collectors for Aqueous High-voltage Batteries. *Chem. Commun.* **2016**, *52*, 10435−10438.

(30) Wang, F.; Lin, Y.; Suo, L.; Fan, X.; Gao, T.; Yang, C.; Han, F.; Qi, Y.; Xu, K.; Wang, C. Stabilizing High Voltage $LiCoO_2$ Cathode in Aqueous Electrolyte with Interphase-forming Additive. *Energy Environ. Sci.* **2016**, *9*, 3666−3673.

(31) Suo, L.; Han, F.; Fan, X.; Liu, H.; Xu, K.; Wang, C. "Water-in-salt" Electrolytes Enable Green and Safe Li-ion Batteries for Large Scale Electric Energy Storage Applications. *J. Mater. Chem. A* **2016**, *4*, 6639−6644.

(32) Zhao, J.; Li, Y.; Peng, X.; Dong, S.; Ma, J.; Cui, G.; Chen, L. High-voltage Zn/$LiMn_{0.8}Fe_{0.2}PO_4$ Aqueous Rechargeable Battery by Virtue of "Water-in-salt" Electrolyte. *Electrochem. Commun.* **2016**, *69*, 6−10.

(33) Chao, D.; Xia, X.; Liu, J.; Fan, Z.; Ng, C.; Lin, J.; Zhang, H.; Shen, Z.; Fan, H. A V_2O_5/conductive-polymer Core/shell Nanobelt Array on Three-dimensional Graphite Foam: A High-rate, Ultrastable, and Freestanding Cathode for Lithium-Ion Batteries. *Adv. Mater.* **2014**, *26*, 5794−5800.

(34) Mendialdua, J.; Casanova, R.; Barbaux, Y. XPS Studies of V_2O_5, V_6O_{13}, VO_2 and V_2O_3. *J. Electron Spectrosc. Relat. Phenom.* **1995**, *71*, 249−261.

(35) Schryvers, D.; Firstov, G.; Seo, J.; Humbeeck, J.; Koval, Y. Unit Cell Determination in CuZr Martensite by Electron Microscopy and X-ray Diffraction. *Scr. Mater.* **1997**, *36*, 1119−1125.

(36) Julien, C.; Massot, M.; Poinsignon, C. Lattice Vibrations of Manganese Oxides: Part I. Periodic Structures. *Spectrochim. Acta, Part A* **2004**, *60*, 689−700.

(37) Babaa, M.; Stepanek, I.; Masenelli-Varlot, K.; Dupont-Pavlovsky, N.; McRae, E.; Bernier, P. Opening of Single-walled Carbon Nanotubes: Evidence Given by Krypton and Xenon Adsorption. *Surf. Sci.* **2003**, *531*, 86−92.

(38) Zhao, T.; Han, C.; Yang, J.; Su, J.; Xu, X.; Li, S.; Xu, L.; Fang, R.; Jiang, H.; Zou, X.; Song, B.; Mai, L.; Zhang, Q. Stable Alkali Metal Ion Intercalation Compounds as Optimized Metal Oxide Nanowire Cathodes for Lithium Batteries. *Nano Lett.* **2015**, *15*, 2180−2185.

(39) Niu, C.; Liu, X.; Meng, J.; Xu, L.; Yan, M.; Wang, X.; Zhang, G.; Liu, Z.; Xu, X.; Mai, L. Three Dimensional V_2O_5/NaV_6O_{15} Hierarchical Heterostructures: Controlled Synthesis and Synergistic Effect Investigated by in Situ X-ray Diffraction. *Nano Energy* **2016**, *27*, 147−156.

DOI: 10.1021/acsami.7b13110
ACS Appl. Mater. Interfaces 2017, 9, 42717−42722